Mem. S.A.It. Vol. 74, 230

**Memorie** della


# Infrared Astronomy with the Hubble Space Telescope and the Next Generation Space Telescope

M. Robberto ⋆

Space Telescope Science Institute, HST Division, 3700 San Martin Drive, Baltimore MD, 21218, USA
e-mail: robberto@stsci.edu

**Abstract.** I review the characteristics of NICMOS before and after the installation of the new cooling system. Recent results on high-redshift supernovae and star formation in the Large Magellanic Cloud are used to illustrate the NICMOS performance. I present the IR channel of WFC3, a fourth generation instrument to be installed on the Hubble Space Telescope in 2004. Finally, I briefly report on the current status of the NGST project.

**Key words.** infrared: general – cosmology: observations – infrared: galaxies – Telescopes: Hubble Space Telescope – instrumentation: spectrographs: NICMOS – instrumentation: detectors: WFC3 – Telescopes: Next generation Space Telescope

## 1. Introduction

When the Hubble Space Telescope was launched in April 1990, it was equipped with five focal plane instruments all able to observe in the ultraviolet (UV) down to $\lambda \leq 1200$ Å. Only one instrument, the Wide-Field/Planetary Camera, could cover the visible range up to the I band. The original goal of the HST program was in fact to put on orbit a 2.4 m telescope optimized for the UV and the visible wavelengths, and the initial complement of instruments coherently exploited the design of the telescope. Little attention, if any, was paid to the behavior of the HST optical assembly at infrared (IR) wavelengths (Robberto et al. 2000).

Twelve years and four Shuttle servicing missions later, the wavelength coverage of HST appears now greatly extended in the visible and near-infrared. The scientific ground of this extension is clear: the expanding Universe shifts to the IR the light emitted in the rest frame at shorter wavelengths. Also, interstellar absorption by dust grains becomes less important at longer wavelengths, making the IR regime the ideal choice for studies of embedded fields, like star-forming regions. The advantages offered in the near-IR by a telescope above the atmosphere are also obvious: diffraction limited imaging with full

*Send offprint requests to*: M. Robberto

⋆ On assignement from the Space Telescope Operation Division of the European Space Agency (ESA).

wavelenght coverage, plus reduced background emission due to the absence of atmospheric airglow lines.

HST had a major impact on IR astronomy. The current near-IR instrument onboard HST, NICMOS, has provided data of unparalleled quality on a number of important fields. NICMOS is based on focal plane arrays originally designed for the HST program. One may remember that in the early '90s the development of the NICMOS's detectors made IR observing routinely available to the general astronomical community, triggering a revolution in IR astronomy.

In this paper, I will summarize the capabilities of the HST in the IR, both existing (NICMOS) and future (WFC3). The performance of NICMOS will be illustrated by a couple of scientific results, whereas for WFC3, still on development phase, only estimates can be given. In the last section I will report on the current status of the Next Generation Space Telescope, the IR-optimized successor of the HST.

## 2. NICMOS

The Near Infrared Camera and Multi-Object Spectrometer (NICMOS) has been installed on the HST during the Second Servicing Mission in February 1997. Principal Investigator has been Rodger Thompson at the Steward Observatory. The instrument was built by Ball Aerospace. NICMOS contains 3 near-IR cameras, each one equipped with its own NICMOS $256 \times 256$ HgCdTe detector. The cameras image simultaneously three fields, almost adjacent, with three different scales (Table 1). Each camera is equipped with 19 optical elements (filters, grism, polarizers) covering the wavelength range from 0.8 $\mu$m to 2.5$\mu$m. Besides imaging, NICMOS allows for slitless grism spectroscopy with $R \sim 200$ in Camera 3, imaging linear polarimetry in Camera 1 and 2, and coronography with $0.3''$occulting spot in Camera 2. A detailed description of NICMOS goes beyond the scope of this review. The reader may check the NICMOS homepage at the URL `http://www.stsci.edu/hst/nicmos`, and in particular the latest version of the NICMOS handbook. Together with a more detailed overview of the instrument, the handbook describes in detail the observing modes currently supported.

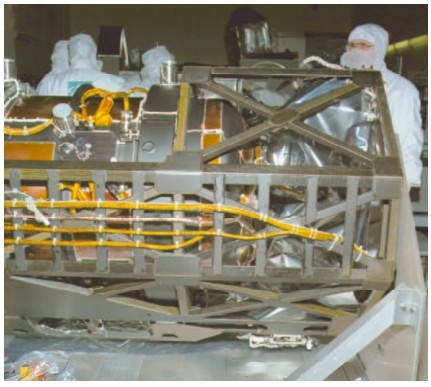

**Fig. 1.** NICMOS during the final tests at Ball Aerospace.

### 2.1. NICMOS cooling: problems and recovery

In NICMOS, the detectors and part of the optical train are installed inside a dewar originally using sublimation of solid Nitrogen. The design lifetime of the coolant was approximately $4.5 \pm 0.5$ years. During the tests before launch (Figure 1), solid Nitrogen was periodically cooled to $\approx 40$ K by flushing Helium through a coil on the back side of the dewar. Unfortunately, this operation caused an unexpected failure. In fact, during the Helium flushing the back side of the solid Nitrogen block was colder than the front side. The resulting cryo-pumping effect transfered the gaseous Nitrogen evaporated on the warmer front side to the back side, where formed extra ice. At the end of the test session, when the dewar was finally allowed to warm up, the extra ice increased its volume and pushed on the inner walls of the dewar. This mechanical distorsion, plastic and permanent,

**Table 1.** Imaging parameters

| Parameter | Camera 1 | Camera 2 | Camera 3 |
|---|---|---|---|
| Pixel Size (arcsec) | 0.043 | 0.075 | 0.2 |
| Field of View arcsec × arcsec | $11 \times 11$ | $19.2 \times 19.2$ | $51.2 \times 51.2$ |
| Diffraction limited wavelength ($\mu$ m) | 1.0 | 1.75 | – |

has produced a number of undesirable effects:

- The three camera are no longer confocal. In particular, NIC3 camera is outside of the focus range correctable with the NICMOS mechanisms, and in order to be used needs a refocussing of the telescope. Since the wide-field Camera 3 does not exploit the resolving power of the HST, the defocussing may be acceptable, depending on the science program. The focus shift between NIC1 and NIC2 is sufficently small that an intermediate focus yields excellent image quality in both cameras.
- The detectors have moved laterally, and there is a $\approx 20$ vignetting in all cameras. The pupil stops are also misaligned and background removal is less than optimal.
- The thermal insulation of the dewar has been compromised. The resulting thermal short has reduced the lifetime of the coolant from 4.5 year to about 2 years.

On January 3, 1999, the cryogen was completely exhausted. This day marks the end of the instrument lifetime under the original cooling regime. After more than three years of inactivity, on March 8, 2002, the astronaut crew of Serving Mission 3B have installed the NICMOS cooling system (NCS), a closed cycle system intented to bring down the temperature of the instrument to $\approx 77$ K (Mackenty & Cheng 1998). Neon gas now flows through the cooling coil originally used to flush liquid Helium. The compresssion-expansion cycle of Neon removes heat from the NICMOS dewar. Heat is transferred to the cryocooler via a heat exchanger, and then transported to an external readiator by the Capillary Pumped Loop. Among the advantages of the NCS one must mention the high operation speed -about 7000 revolution per second- which is ideal to minimize vibrations.

### *2.2. NICMOS today*

The first test images taken with the refurbished NICMOS demonstrate that the instrument is again fully operational. Performance is actually improved. Since the NCS allows the detector to operate at a temperature slightly higher than with the original cooling system, the quantum efficiency turns out to be higher without the price of a significant increase of dark current. Early tests show that a faint objects with $m_{AB} = 22$ over 1 arcsec$^2$ at $1.6\mu$ m in NIC2, F110W, now provides S/N=36, against a S/N=27 before the installation of the NCS. Scientific observations have resumed in middle June 2002, and there is a general agreement between the calibration data and the performance predicted with the latest version of Exposure Time Calculator, available on the URL: `http://stsdas.stsci.edu/ETC/NIC/nic_img_etc.html`.

## 3. Science with NICMOS

In is beyond the scope of this paper to account for the scientific discoveries made by NICMOS. I will highlight only a few results, selected to provide an overview of the instrument's capabilities.

### 3.1. Accelerating universe

Type Ia supernovae (SNe Ia) are standard candles, i.e their apparent brightness allows to obtain an accurate measure of the distance of the host galaxies. By combining distance with red-shift, one can verify if the rate of expansion of the Universe is constant over time. The fact that at redshift $z \simeq 0.5$ SNe Ia are fainter than expected provides a strong indication that the Universe is now accelerating. Models predict that acceleration follows a previous deceleration phase, and therefore supernovae at largest redshifts are needed to confirm our confirm our understanding and constrain the basic cosmological parameters. Supernovae at larger reshifts are expected to peak in the near-IR. They are extremely faint (at $z = 1.6$ they have $m \approx 24$ in J and H) and require extremely stable photometric conditions in order to measure with high accuracy their brightness on top of the host galaxy. The absence of atmospheric seeing, together with the stability of the PSF over long time-scales, makes this an ideal field of application of NICMOS.

SN 1997ff is the furthest SN Ia observed to date, at a redshift $z \approx 1.7$. It was discovered during the repeated observations of the Hubble Deep Field-North, and serendipitously monitored with NICMOS during the GTO campaign (Thompson et al. 1999). The NICMOS data (Figure 4) (Riess et al. 2001) have constrained the redshift at $z = 1.7 \pm 0.1$, and the brightness is consistent with an earlied decelerating universe with cosmologial parameters $\Omega_M \approx 0.3$ and $\Omega_\Lambda \approx 2/3$. Various astrophysical phenomena have been invoked to explain the apparent accelaration of the universe, but the NICMOS results seem to rule them out, confirming that the acceleration is real and due to some form of "dark energy".

### 3.2. Star Formation in the LMC

The Large Magellanic Cloud, with an average metallicity $Z \simeq 0.3\ Z_\odot$, hosts a rich variety of star-forming regions of different age and stellar composition. The most spectacular field is certainly the giant complex of HII regions 30 Dor. Interpreted for a long time as a rather uninteresting evolved HII region, 30 Dor is now considered a milestone in our understanding of the formation and very early evolution of massive stars. The region is the most active site of massive star formation within the Local Group, and the nearest example of the more distant and unresolved starbursts.

The 30 Dor region is powered by R136, a 2Myr old massive cluster. The entire area is extremely crowded and the superb image quality of NICMOS, with PSF almost constant over an extended field of view, is required to obtain IR data with quality comparable to that obtained in the visible also by HST. The NICMOS data (Walborn et al. 1999) show that a "second generation" of star formation is triggered by the R136. Many new IR sources, including multiple systems, clusters, and nebular structures, are found in the periphery of R136 (Figure 3). Dust pillars with O stars at the top are visible, oriented directly toward R136. This provides strong support to the hypothesis that triggered star formation may occur at the heads of dust pillars. The higher mass density associated with the local star formation episode on top of the pillars shields the neutral material lying behind from the advancing main ionization front, actually creating the pillars. The detection of jets from massive stars is also important, as it indicates that disk-accretion still occurs around newly formed, visible massive star. There are only a few known cases of massive young stars powering bipolar outflows within the Galaxy.

## 4. The Wide Field Camera 3 (WFC3)

Wide Field Camera 3 will be installed on the HST in 2004 during Servicing Mission 4. Unlike the preceeding instruments, WFC3 is "internally" built by a team of astronomers and engineers from NASA, STScI, JPL, and industrial conc-

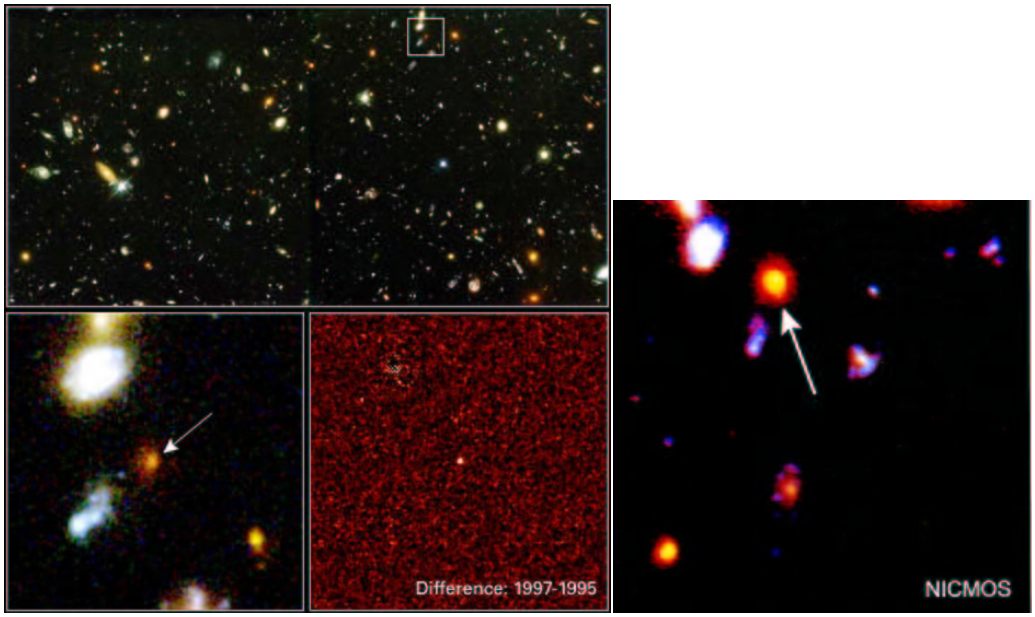


**Fig. 2.** Left panel: WFPC2 images of 1) portion of the HDF-North where SN 1997ff has been located (top); 2) close up of the white box area, with the white arrow pointing to the host galaxy. Its redness is due to the billions of old stars residing there (bottom left); 3) difference of two frames taken two years apart showing the SN (bottom right). Right panel: color-composite images of the same region taken NICMOS images. Note that the field here is sligthly rotated with respect to the WFPC2 images.

tractors, mainly Ball (BASD) , with an independent oversight commitee appointed by NASA representing the worldwide astonomical community. WFC3 (Figure 4) has two independent channels, one for the UV and visible wavelengths (UVIS, $\approx$ 2000 Å to 1$\mu$m) and the other for the near-IR wavelengts (IR, $\approx$ 0.8 to 1.7 $\mu$m). The UVIS channel is based on a pair of butted 4K$\times$2K thinned, back illuminated CCDs produced by Marconi (UK), whereas the IR channel is based on a new HgCdTe detector 1K$\times$1K made by Rockwell Science Center. The IR channel has a scale of approximately $0\farcs121 \times 0\farcs135$/pixel, with a field $\approx 127'' \times 137''$. The rectangular shape is due to the detector tilt with respect to the chief ray caused by the off-axis optical design.

The two channels view the same on-axis field, but not simultaneously; a channel selection mechanism diverts the beam to one or the other channel. The optical design of the IR channel is all-reflective, with the exception of a lens performing the spherical aberration correction at the cold pupil. The cooling system is based on termoelectric coolers (TECs). While TECs provide virtually unlimited cooling capability, the price is reduced cooling power. The operating temperature of the IR detector will be, in fact, close to 150 K, much higher than $T \approx 77$ K of NICMOS. At 150 K, conventional HgCdTe devices with cut-off at $\approx 2.5$ $\mu$m generate an intolerably high dark current. Since the dark current is related to the bandgap, by shortening the cutoff wavelengths to $\approx 1.7\mu$m it is possible to keep the dark current below the natural limit imposed by the average zodiacal background, estimated in approximately 0.2 electrons/second/pixel.

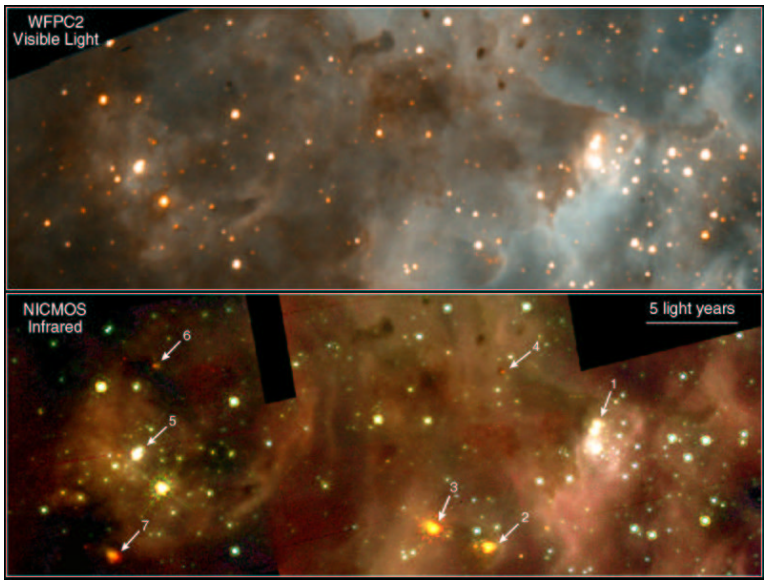


**Fig. 3. Upper Panel**: WFPC2 F336W, F555W, F814W (blue, green, red, respectively) composite of a field in the 30 Doradus region. Note the location of the triple stellar system (Knot 1) at the apex of a large dust pillar, whose summit has been blown off; the pillar is oriented toward R136, outside the field to the SW of Knot 1. Note also the "inverted Y" configuration of four prominent dark globules north of Knot 1. **Lower Panel**: NICMOS J, H, K (blue, green, red, respectively) composite of the same field. Note the faint, very red object within the easternmost of the four dark globules north of Knot 1.

This constrains defines the long wavelength cutoff of WFC3.

The IR filter wheel accomodates 15 passband filters, two grisms and a blanck position, including broad-band filters, medium-band filters centered on molecular features and nearby continuum, and narrow-band filters probing interstellar diagnostic lines.

Up to 1.7$\mu$m, WFC3 offers a 6.4 larger field of view of NICMOS/Camera 3 with substantially better spatial sampling and sensitivity, this last depending on the final detector performance. According to the most recent predictions, WFC3 will reach S/N=5 in 10 hr for a point source with H=26.3. An exposure time calculator is mantained at the STScI with the most recent values for the instrument throughput, filter transmission and detector performances. It is fount at the URL: `http://www.stsci.edu/instruments.wfc3.etc-list.html`.

## 5. The Next Generation Space Telescope (NGST)

Like HST, the Next Generation Space Telescope is a collaborative effort between NASA and ESA, joined by the Canadian Space Agency. The development of the project is lead by the NASA's Goddard Space Flight Center. The Space Telescope Science Institute is responsible for the Science and Operation Center.

The goal of NGST is to directly attach the most fundamental open questions of contemporary astrophysics: what is the history and the structure of the Universe? How galaxies form and evolve? What is the history of our Galaxy? How stars, brown dwarfs, and planetary systems form? What

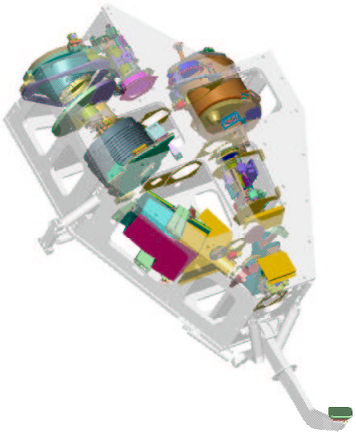

**Fig. 4.** Schematic of the WFC3 optical bench. The light from the secondary mirror is intercepted by the pick-off mirror protruding at the bottom of the figure, then enters the optical bench where immediately encounters the channel selection mechanism. A mirror can be placed to reflect the beam to the IR channel. In the figure the UVIS channel is on the left, the IR channel is on the right.

is the nature of dark matter? Such an ambitious task requires extreme design parameters:

- 6m class mirror, lighweight and deployable;
- Telescope passively cooled by large sunshade;
- Second Lagrange Point (L2) of Earth-Sun system orbit;
- Image quality diffraction limited (Strehl ratio=0.8) at 2 $\mu$m;
- wavelength range 0.6-10 $\mu$m, with zodiacal-light-limited performance, instrument limited up to 20 $\mu$m;
- imaging and spectroscopic instrumentation over the wavelength range;
- 5 year minimum lifetime, 10 year goal.

As for today (June 2002) two proposals are competing to be the prime-contractor of NGST: TRW/Ball (Figure 5) and Lockheed-Martin (Figure 6). The selection is expected at the end of summer 2002. NGST will be equipped with three instruments, housed in the Integrated Science Instrument Module (ISIM): the near-IR camera (NIRCam), the near-IR spectrom-

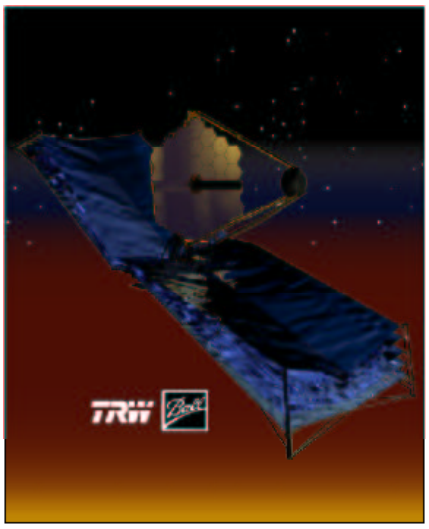


**Fig. 5.** TRW/Ball concept of the NGST telescope

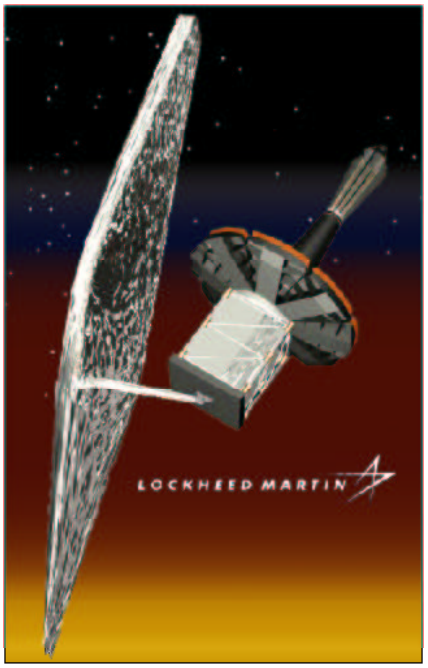


**Fig. 6.** Lockheed-Martin concept of the NGST telescope

eter (NIRSpec) and the mid-IR instrument (MIRI), plus the guide system. The consortia building the instruments have been recently selected:

- NIRCam will be built by a a team lead by the University of Arizona (lead investigator Marcia Rieke);
- NIRSpec will be built by ESA with a primarily European science team;
- MIRI will be build in a 50/50 collaboration between NASA and individual European nation states, managed by ESA. US lead implementing center is JPL (Instrument Scientist Gene Serabyn), whereas the US science team is lead by G. Rieke.

The NGST guider will be provided by Canada.

### 5.1. NIRCam

NIRCam is the imaging instrument for the wavelength range $\sim 0.6-5$ $\mu$m. The instrument is composed by 4 modules: two for imaging and two for imaging spectroscopy through tunable filters. The two imaging modules are identical, so that the field of view can be maximized within the reliability and cost constrains of the NGST project. Light entering each imaging module si splitted by a dichroic in two optical arms: a short wavelength arm ($\lambda \leq$ 2.5 $\mu$m) and a long wavelength arm ($\lambda \geq$ 2.5 $\mu$m). They observe the same field with different spatial resolution: one is Nyquist-sampled at 2 $\mu$m, providing $0\farcs034$/pixel, on a 4k×4K detector, the other is Nyquist-sampled at 4 $\mu$m and delivers $0\farcs068$/pixel on a $2K\times$2K detector. The resulting field of view in both cases is $2.3' \times 4.6'$, which doubles when the other imaging module is considered. The two imaging modules dedicated to imaging spectroscopy are dedicated one to the short wavelengths (1.2-2.5 $\mu$m) and the other to the long wavelengths (2.5-45 $\mu$m). The spatial scale is $0\farcs068$/pixel and the spectral resolution of $\approx$ 1%. Moreover, all modules have a coronographic mode, with a spot on the focal plane and a coronographic mask on the pupil wheel. Used in conjunction with the tunable filters, the coronographic mode will allow e.g. to obtain low resolution spectra of faint objects near bright stars (e.g. exoplanets).

The expected point-source sensitivity, S/N=10 in broad band imaging (R=5), is of the order of a few nJy in 100,000 seconds. Further informations can be obtained at the URL:
`http://ircamera.as.arizona.edu/nircam`

### 5.2. NIRSpec

NIRSpec will cover the wavelength range $\sim 0.6-5$ $\mu$m with resolving power $\sim$ 100 and $\sim$ 1000. The design will take advantage of an innovative Micro-Electromechanical System (MEMS), namely a micro-shutter array. This will allow the user simultaneously observe hundreds of objects through the opening of an array of micro-shutters located at the focal plane. It has been recently decided to proceed with the micro-shutter technology rather than with the similar micro-mirror approach, where the shutters operate in reflection rather than in transmission. The projected pixel size will be approximately 100mas, and the sensitivity, S/N in 100,000 at R=1,000, will be of the order of a fraction of a $\mu$Jy.

Further informations can be obtained at the URL:
`http://astro.estec.esa.nl/NGST`

### 5.3. MIRI

MIRI will provide imaging and spectroscopy between 5 and 28$\mu$m. The functional requirements made by the Mid-Infrared Steering Committee are:

- Wavelength range 5-25 $\mu$m, possibly up to 28.2 $\mu$m in order to cover an important emission line of $H_2$;
- Diffraction limited optics over the entire wavelength range and large field size.

Pixel size $\sim 0\farcs12$/pixel, field $\sim 2 \times 2$ arcmin;
- Coronographic imaging capability;
- Spectroscopic mode with $R \sim 100$ in the range 5-10 $\mu$m;
- Integral field spectroscopy with $R \sim 1000 - 2000$ with pixel size $\sim 0\farcs2$ and $\sim 0\farcs4$ over a field of view of $\sim 2 \times 2$ arcmin;
- Lifetime 10 years.

The proposed agreement between NASA and ESA assigns to the European part the responsability for the optical and mechanical/cryogenic parts; the US team will be responsible for the detectors and electronics, system integration, calibration, etc.

### 5.4. NGST Detectors

A m=33 source observed with the NGST will provide less than 1 photon/second on the detector. In order to be detected such low flux, it is necessary to couple the extraordinaly low background conditions of the L2 site with a new generation of IR detectors having extremely low noise. These detectors are under development at the Rockwell Science Center (1-5 $\mu$m HgCdTe technology), in collaboration with the team of D. Hall at the University of Hawaii; at Raitheon Infrared Operations (InSb technology) in collaboration with the team of W. Forrest at the University of Rochester, and at the NASA Ames Research Center, where the team of C. McCreight is developing and characterizing Si:As mid-IR detectors. A fourth laboratory, the Indepenent Detector Testing Laboratory (IDTL, PI D. Figer) has been funded at STScI to characterized both HgCdTe and InSb detectors in a comparative hardware setup.

The detector technology for the 1-5 $\mu$m channel will be selected in the summer 2003.

## 6. Conclusions

As a final remark, let me underline that through the ESA partecipation both the HST and the NGST are facilities open to the European scientific community. Staff at the STScI and at the ECF can be contacted for further informations about instrument performance, observing time application and data mining in the huge and publicly available archive of HST data.

*Acknowledgements.* I'm indepted to my collegues of the Space Telescope Science Institute, in particular J. MacKenty, M. Stiavelli and D. Calzetti, for our daily exchange of ideas on the topics of this paper. Thanks to the organizers of this interesting meeting and to S. Ciprini of the LOC for his help editing this constribution. I take this opportunity to aknowledge Prof. Maffei for his books, my early readings on astronomy, that inspired me when I was a teenager.

## References

MacKenty, J. W. & Cheng, E. S. 1995, in NICMOS and the VLT: A New Era of High Resolution Near Infrared Imaging and Spectroscopy, ESO Conference and Workshop Proceedings 55, Wolfram Freudling and Richard Hook eds.,p.214

Riess A. G., Nugent P. E., Gilliland R. L., Schmidt B. P., Tonry J., Dickinson M., Thompson R. I., Budavari T., Casertano S., Evans A. S., Filippenko A. V., Livio M., Sanders D. B., Shapley A. E., Spinrad H., Steidel C. C., Stern D., Surace J., & Veilleux S. 2001, ApJ 560, 49

Robberto, M., Sivaramakrishnan, A., Bacinski, J. J., Calzetti, D., Krist, J. E., MacKenty, J. W., Piquero, J., & Stiavelli, M. 2000, in UV, Optical, and IR Space Telescopes and Instruments, Proc. SPIE Vol. 4013, J. B. Breckinridge and P. Jakobsen Eds., p. 386

Thompson, R. I., Storrie-Lombardi, L. J., Weymann, R. J., Rieke, M. J., Schneider, G., Stobie, E., & Lytle, D. 1999, AJ, 117, 17

Walborn, N. R., Barbá, R. H., Brandner, W., Rubio, M., Grebel, E. K., & Probst, R. G. 1999, AJ, 117, 22